Display
CLM - P 268

CLM - P 268

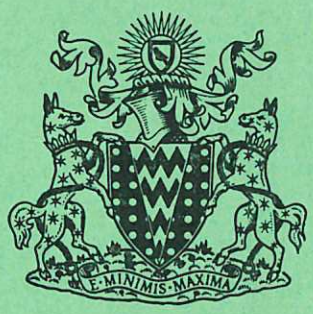

United Kingdom Atomic Energy Authority
RESEARCH GROUP
Preprint

THE ION AND VELOCITY STRUCTURE IN A LASER-PRODUCED PLASMA

F. E. IRONS
R. W. P. McWHIRTER
N. J. PEACOCK

Culham Laboratory
Abingdon Berkshire

1971

CLM - P 268

THE ION AND VELOCITY STRUCTURE IN A LASER-PRODUCED PLASMA

by

F.E. Irons, R.W.P. McWhirter[*], and N.J. Peacock

(Submitted for publication in J. Phys. B: Atom. Molec. Phys.)

A B S T R A C T

The early expansion of a plasma produced by the laser irradiation of a polyethylene foil in vacuum has been studied by making observations at right angles to the target normal. Spectral line emission has been scanned to give the spatial distribution of the ions C I - VI. Certain spectral lines are predominantly Doppler broadened by the ion streaming motion and this broadening has been interpreted to give velocity as a function of distance from the target normal. Flight paths have been deduced for the C V ions, and velocities along the paths have been calculated. Doppler shifts have also been observed parallel to the target normal and are in agreement with previous time-of-flight measurements.

[*] Astrophysics Research Unit, Science Research Council, Culham Laboratory, Abingdon, Berks.

U.K.A.E.A. Research Group,
Culham Laboratory,
Abingdon,
Berks.,
England.

May 1971

C O N T E N T S

1. Introduction

When a high power Q-spoiled laser pulse is focussed onto an extended material surface in vacuum, a plume of plasma is formed, which is highly ionized and which expands away from the material surface with a distribution of velocities of up to 10^7 cm s^{-1}. The gas dynamic phase of the expansion has been studied by many authors, usually by means of particle detectors at distances greater than about 10 cm from the target surface. These studies, for laser powers greater than about 100 MW , have included (i) the measurement of average expansion velocities for a wide range of elements by the time-of-flight technique, as a function of laser power and of angle to the target normal (Opower et al. 1965, 1966, 1967; Gregg and Thomas, 1966; Sucov et al. 1967; Bykovskii et al. 1968); (ii) the measurement of the velocity spectrum of individual ion species (Langer et al. 1966; Tonon and Rabeau, 1969; Bykovskii et al. 1969a; Demtröder et al. 1970); and (iii) the measurement of the angular ion distribution (Opower and Press, 1966; Langer et al. 1966; Bykovskii et al. 1969b).

Spectroscopic techniques have been employed to study the plasma expansion in the region of a few cm from the target surface. Shadowgraphs and luminosity photographs, with nanosecond exposures, show the shape of the plasma as a function of time (Fabre et al. 1966; Sucov et al. 1967; Basov et al. 1968; Tonon and Rabeau, 1969). These, and streak photographs (Weichel and Avizonis, 1966; Basov et al. 1966) enable the velocity of the leading edge of the plasma to be calculated. In a few cases the light emission from the plasma has been spectrally resolved and velocities of individual ion species have been measured from the time-of-flight of line radiation

(Boland et al. 1968, to be referred to henceforth as paper I; Basov et al. 1969; Dhez et al. 1969). The above quoted papers show that the more highly stripped ions have the higher mean energy; that, in most cases, the normal to the target surface is an axis of symmetry of the plasma expansion and that the ions are concentrated about this axis, though the shape of this concentration can vary, depending on the laser power.

The present paper is concerned with the plasma formed when a Q-switched ruby laser pulse of energy 5 J and half width 17 ns is focussed onto a polyethylene foil in vacuum. Spectral line emission from the plasma has been measured by making observations at right angles to the target normal. Measurements are reported of the spatial distribution of intensities of lines of C I - VI, and of velocities derived from Doppler shifts in the same lines. These two sets of measurements, when combined, give the velocity as a function of distance from the target normal. They also lead to the construction of a map of ion flight paths, in the case of the line C V 2271 Å, which is considered in some detail. The above measurements cover the region 0.35 to 5.0 mm from the target surface. An observation of Doppler shifts in light emitted parallel to the target normal is also reported, and the resulting velocities are found to be in agreement with values previously obtained from the time-of-flight of line radiation (paper I).

A knowledge of the spatial and velocity distribution of the different ion species is important to any practical application of the plasma as an ion source (Bykovskii et al. 1968; Tonon and Rabeau, 1969; Eloy, 1969; Peacock and Pease, 1969), and also because it leads to an improved understanding of the laser-plasma interaction (e.g. Dawson et al. 1969). Also, the increasing use of the laser-produced plasma as a source of line radiation for level classifications,

makes it essential to know what structure is likely to be present in the line profiles (e.g. Valero et al. 1969).

2. Experimental Arrangement

A Korad K1500 ruby laser system was Q-switched to give an output of 5 J in a pulse of duration 17 nanoseconds at half maximum. The beam was focussed into a vacuum chamber at 10^{-4} torr by a lens of focal length 10 cm, so as to fall at normal incidence onto a polyethylene $(C_2H_4)_n$ foil, 0.25 mm thick. About 70% of the laser power was focussed within a circular spot of diameter 0.3 mm giving an average light flux of 2.9×10^{11} watts cm^{-2}. Light from the plasma so formed was focussed by a quartz-lithium fluoride achromat onto the entrance slit of a 1.5 m focal length Ebert monochromator, the signal at the exit slit being monitored by a photomultiplier (EMI 9594 QB) and then displayed on a Tektronix 519 oscilloscope. The monochromator had a single channel and profiles were built up on a shot-to-shot basis. The instrumental risetime of the system was measured to be ~ 3 ns. The experimental arrangement is the same as that used in paper I and reference can be made to that paper both for further experimental details and for details of the plasma itself.

Time is measured from the time of arrival of the leading edge of the laser pulse at the target surface, and on this time scale, the time of the laser peak intensity corresponds to $t = 20$ ns.

3. Space Scans and Line Profiles

In paper I, a spectroscopic study of the plasma expansion in the direction of the target normal was reported. This has included measurements of the temperature and density as a function of distance from the target surface, and measurements of velocity from the time-

of-flight of line radiation. The present paper is concerned with the component of the expansion at right angles to the target normal, as revealed by the distribution of spectral line emission in space and by spectral line broadening.

The spectral line broadening has contributions from both Stark and Doppler broadening. Stark broadening, which is the subject of a separate paper (Irons, 1971), is the dominant broadening mechanism in some lines close to the target surface where the density is highest (see e.g. the lower spectrum in Fig.7). It decreases rapidly with distance from the target surface and is readily distinguishable from Doppler broadening which is fairly constant with distance. In this paper we are concerned with lines in which Doppler broadening is dominant, at least beyond about 1 mm from the target surface. The Doppler broadening is interpreted on the basis of ion streaming, and this is seen to give consistent results; i.e. the contribution to the line broadening by thermal motion is assumed to be small (Allen (1970) has found the ion temperature to be comparable to the electron temperature, in which case this assumption is justified).

3.1 The measurement of space scans and line profiles

The particular lines chosen for the measurements are listed in Table 1. These have been chosen because their Doppler broadening is greater than their Stark broadening and their fine structure separation, and because they have suitably high intensity (to compromise between line intensity, which decreases with distance, and the excessive background continuum which exists near the target surface, it was necessary to make the measurements at a distance of 1.6 mm from the target surface).

Table 1

Line	Ion to which the line refers
C VI 2070 Å	C^{6+}
C V 2271	C^{5+}
-	C^{4+}
C III 4187	C^{3+}
C II 4267	C^{2+}
C I 2479	C^{1+}

Unfortunately there was no suitable line for C IV; and the line C VI 2070 Å still has Stark broadening comparable to Doppler, though less so than other C VI lines. Each line in Table 1 originates from a level which is collision coupled to the next ion stage, so that the line should be identified with that ion, as indicated in the second column (see paper I for an explanation of this point).

The plasma is formed at the focal point of the laser beam and streams away from this point with some distribution about the target normal. The target normal at the focal spot, which also is the axis of the laser beam, will be referred to as the x axis: the target surface lies in the y, z plane, with the z axis pointing towards the viewing monochromator (see Fig.8). Line (wavelength) profiles were measured with the plasma viewed along the z coordinate i.e. at y = 0, the monochromator bandwidth being chosen small compared to any structure in the line profile. For the space scans the line emission was scanned up and down the y-coordinate, the plasma being viewed parallel to the z-coordinate and with the monochromator bandwidth being set

to record a wavelength band (smaller than the line width) at the line centre, thereby collecting light from only those parts of the plasma moving at right angles to the line of sight. With the plasma assumed to be symmetrical about the x axis, the distribution measured along the y coordinate is representative of any direction at right angles to the x axis.

The space scans and line profiles were built up on a shot-to-shot basis, with typically two or three shots being recorded at each of some thirty positions across the profiles, and examples are shown in Fig.1. In this figure the data for two or three shots recorded at each position have been joined by vertical lines to give an indication of the shot-to-shot spread in intensity. A smooth curve has been drawn to give a visual best fit to the experimental points. All the curves to be presented later in Figs.2-5 are visual best fits derived in this way. The instrumental full width is 0.30 Å.

The consistency of the Doppler interpretation of the line profiles is taken to mean that opacity effects do not strongly influence the line profiles, e.g. for lines of the same ion the broadening scales with wavelength, and where a line is sufficiently intense to be observed out to 12 mm from the target surface, the shape of the line profile remains fairly constant even though the density has decreased by five orders of magnitude. The fact that the ions are moving relative to one another in a non-thermal manner makes it difficult to calculate the magnitude of the opacity effect.

3.2 On the interpretation of the space scans and line profiles

The component of velocity observed at right angles to

the target normal, is related to distance from the target normal. This means that each point in a space scan and a line profile is weighted according to the depth increment of plasma which emits light within the velocity increment acceptable, via the Doppler effect, to the monochromator bandwidth. The depth increment may vary across the space scan and line profile, and these may therefore suffer a distortion. A full analysis of this effect would require a precise knowledge of the velocity-distance relationship and is outside the scope of this paper. Instead, the space scans and line profiles are presented as measured; a model is considered (section 5.1), and an analysis based on this model shows that the measurements give useful mean values as they stand.

4. Results

Characteristic of the measurements of space scans and line profiles are those of the line C V 2271 at x = 1.6 mm, to be described first in some detail (section 4.1). Following this, similar measurements for C I-VI at x = 1.6 mm are presented to show the distribution of these ion species in space and the distribution of velocity at right angles to the x axis (section 4.2). The line C V 2271 has been observed at distances x = 0.35 - 5.0 mm to show the distribution and velocity of this ion, both parallel to and at right angles to the x axis (section 4.3). Finally there is a brief section on the Doppler shift in light emitted parallel to the x axis (section 4.4).

4.1 C V 2271 at x = 1.6 mm

Figure 2 shows sets of space scans and line profiles of C V 2271 at x = 1.6 mm, arranged as a time sequence. Both sets are symmetrical,

which reflects the circular symmetry which is assumed to be present about the x axis. Early in time the space scans show that the majority of C V ions lie in two regions, which in circular symmetry would be parts of an annulus centred on the x axis (see Fig.8), and the well defined Doppler shifted peaks shown by the line profile indicate that these regions are moving away from the x axis, one towards and one away from the observer. The wavelength displacement of the line peak gives a mean velocity for the plasma whose distance from the x axis is given by the spatial displacement of the line peak, e.g. at t = 30 ns the line shift is 0.85 Å (half the peak-to-peak displacement) and this gives a mean velocity of 1.1×10^7 cm s^{-1} for the plasma at a distance of 1.5 mm from the x axis (half the peak-to-peak distance). The small spectral width of the line peak structure indicates that there is a relatively small spread of velocity about the mean value. At later times the light emission becomes more concentrated about the x axis and the line shift and velocity become smaller.

It is interesting to note that an integration in time of the line profiles in Fig.2 would produce a square shaped profile, the edge and centre of the square being composed of light from early and late in time respectively. This explains the square shaped profile observed for this line in photographs of the spectrum.

4.2 C I - VI at x = 1.6 mm

Space scans and line profiles of the lines in Table 1 have been recorded at x = 1.6 mm, and examples of these have been shown in Fig.1. In Fig.3 space scans of each line have been plotted together on a common abscissa and arranged as a time sequence, with the peak intensity of each line in time normalised to unity. It can be seen

from this figure that the highest ion stages appear first and are followed at later times and at greater distances from the x axis by ions of successively lower degrees of ionization. Although each line when it first appears is displaced from the x axis, this displacement decreases with time and towards extinction each line peaks on axis. Exceptions are C I and II which show a second peak towards extinction.

The wavelength profiles of C III, II and I were found to follow the trend of C V in Fig.2, viz. to show two peaks displaced from the line centre early in time, merging into one peak at the line centre later in time. Mean velocities were calculated from the wavelength displacement of the line peaks and were related to the plasma at distances given by the spatial displacement of the line peaks (as described in section 4.1). This leads to the plots of mean velocity against distance in Fig.4. The error bars shown in this figure arise from the uncertainty in locating the various peaks and represent about 80% confidence limits.

The space scans and line profiles of C VI also show a tendency to peak. This reflects the increase in electron temperature approaching the x axis, but unlike C V-I it does not represent the highest concentration of the ion. Unfortunately a Stark contribution to the broadening smooths out some of the peak structure of C VI and the points plotted for this line are only approximate values.

4.3 C V 2271 at x = 0.35 - 5.0 mm

Because of its high intensity and minimal Stark broadening, the line C V 2271 has lent itself to observations over an extended distance. Space scans and line profiles were recorded at x = 0.35, 0.65, 1.0, 1.6, 2.8 and 5.0 mm, and were all found to follow the trend of

those shown in Fig.2 for x = 1.6 mm. One space scan from each distance, for the time t = 45 ns, is plotted in Fig.5 and shows that in the x, y plane the C V emission occupies a V-shaped region, with the point of the V towards the focal spot. A useful way of presenting this data, and similar data at other times is to plot half the peak-to-peak separation as a function of x. Fig.6(a) shows such a plot, for the times t = 15(10)65 ns, indicated on the plot by brackets, with the points at each time being replaced by a smooth curve. The numbers without brackets give values of the mean velocity away from the x axis, calculated from half the wavelength spacing of the peaks in the line profiles.

4.4 Doppler shift parallel to the target normal

It is appropriate to report one further observation; namely, a Doppler shift in light emitted parallel to the target normal. To observe such a shift a quartz disc was placed on the x axis, 20 cm from the target surface, set at the Brewster angle so as to pass the laser beam unattenuated, but to reflect a fraction of the plasma light through a lens and onto the entrance slit of a spectrograph. A spectrum was recorded on 70 shots of the laser and portions of this spectrum containing lines of C I, IV, V and VI are shown in Fig.7 (the upper spectrum). On the same plate a second spectrum was recorded, but with the plasma viewed at right angles to the target normal (the lower spectrum in Fig.7). The latter contains lines which, though broadened, have no nett shift and therefore provide a reference against which shifts in the former can be measured.

A shift in the lines of C VI, V and IV is clearly visible in the upper spectrum of Fig.7 relative to the lower spectrum, while any shift in C I is smaller than the experimental resolution. The line

shifts and the corresponding velocities are shown in Table 2.

Table 2

Velocities along the target normal

Line	Line shift	Velocity Doppler	Velocity: time of flight (Boland et al. 1968)
C VI 3434	2.8 ± 0.8 Å	$2.4 \pm 0.7 \times 10^7$ cm s^{-1}	$3.3 \pm 0.7 \times 10^7$ cm s^{-1}
C V 2982	2.2 ± 0.6	2.2 ± 0.7 "	3.1 ± 0.7 "
C IV 2530	1.8 ± 0.6	2.1 ± 0.7 "	2.5 ± 0.5 "

Also included in Table 2 are the velocities measured from the time-of-flight of line radiation parallel to the x axis (paper I). These agree with the Doppler values within the experimental uncertainty. The shifts in the lines of C III, II and I were smaller than the experimental resolution and the upper limits which this sets on the ion velocities are consistent with the time-of-flight measurements.

5. Discussion

Measurements of space scans and line profiles of C I-VI have been described in sections 4.1 and 4.2 and have been interpreted to give the plots of velocity versus distance in Fig.4. This interpretation is now discussed (section 5.1). The measurements on C V over the region x = 0.35 - 5.0 mm, summarised in Fig.6(a), are further interpreted to yield the flight paths of individual C V ions (section 5.2). Finally a picture is presented of the distribution of C V throughout the plasma (section 5.3).

5.1 The velocity distribution at right angles to the target normal

The points in Fig.4 indicate the distribution of mean velocity at right angles to the target normal. These were derived from the peaks in the space scans and line profiles, which, as pointed out in section 3.2. may be distorted by the monochromator bandwidth not seeing a uniform depth of plasma over the profiles. It is the aim of this section to investigate this effect; and to this end a model has been taken for the velocity distribution. The model chosen is the simplest which is consistent with the observation that the space scans and line profile are similar in form, viz. it takes the velocity perpendicular to the x-axis, $v(r)$, to be a single valued function of the distance r from the x-axis.

For the space scans, on the above model, it can easily be shown from geometrical considerations that the monochromator of bandwidth $\Delta\lambda$ at the line centre, viewing the plasma at a distance y from the x-axis, sees plasma from a depth δz, where $\frac{\Delta\lambda}{\lambda_o} = \frac{v}{r}\frac{\delta z}{c}$ and $r = \left(\frac{\delta z^2}{4}^{o} + y^2\right)^{\frac{1}{2}}$. Hence the monochromator with a constant bandwidth $\Delta\lambda$ would see a constant plasma depth δz across the space scan only if $\frac{v}{r}$ is constant. For the line profiles, the monochromator, centred at say, λ sees plasma of velocity v where $\frac{\lambda - \lambda_o}{\lambda_o} = \frac{v}{c}$; and then taking increments, a bandwidth $\Delta\lambda$ would see a velocity increment Δv where $\frac{\Delta\lambda}{\lambda_o} = \frac{\Delta v}{c}$ or $= \frac{dv}{dr}\cdot\frac{\Delta r}{c}$. Hence the monochromator with a constant bandwidth $\Delta\lambda$ would see a constant plasma depth Δr over the line profile only if $\frac{dv}{dr}$ is constant.

The functions $\frac{v}{r}$ and $\frac{dv}{dr}$ were calculated to a first approximation from a curve drawn through the velocity points in Fig.4, and were then used to modify the space scans and line profiles, leading to a revised set of velocity points. After a series of successive approximations a final form for $v(r)$ was arrived at which was

consistent with the measurements and this is shown in Fig.4 for the two graphs which contain the largest number of experimental points (t = 40 and 50 μs). The final form for $v(r)$ was almost linear with r which means that the factors $\frac{v}{r}$ and $\frac{dv}{dr}$ are almost constant, and that therefore the space scans and line profiles are not seriously distorted. Indeed the points in Fig.4 as they stand give a fair representation of the function $v(r)$.

The actual ion velocities in the plasma may be distributed about a mean value, rather than be single valued as in the above model, and the points in Fig.4, as they stand, should give a useful measurement of the mean velocity as a function of distance.

5.2 C V ion flight paths and velocities

The curves in Fig.6(a) show the location of the C V peak emission at intervals of 10 ns. In paper I it was concluded from experiment that although recombination of C VI to C V is important between x = 0 - 1 mm, it could be neglected between x = 1 - 5 mm, and this conclusion was supported by theoretical calculations of the collisional-radiative decay coefficient. Similar calculations showed that there was negligible recombination of C V to C IV. It is concluded therefore that beyond x = 1 mm the curves in Fig.6(a) represent the positions of the same C V ions at intervals of 10 ns. Additional curves are available for times Δt = 5 ns intermediate between those shown in Fig.6(a). A C V ion at x = 1 mm at, say t = 35 ns would travel away from the x axis a distance of 0.5 mm (calculated from the average of the velocities at t = 35 and 40 ns) onto the t = 40 ns curve at x = 2.9 mm and then, onto the t = 45 ns curve at x = 4.9 mm, and so on. Flight paths calculated in this way are shown in Fig.6(b) for ions starting at

x = 1 mm at t = 25(5)55 ns: the circles along the various paths represent the points of calculation at 5 ns intervals. Also marked on each flight path is the particle velocity along the path.

Each flight path is an approximate straight line, and when extrapolated back to the target surface, x = 0 mm, would appear to originate from within the focal area. The velocity along each path is fairly uniform out to x = 5 mm and the component of velocity parallel to the x axis has a time averaged value of $\sim 3.0 \times 10^7$ cm s^{-1} which is in good agreement with the values in Table 2.

The velocities are also fairly constant in time, from t = 25 to 50 ns and this is in contradiction to the one dimensional theory of the plasma expansion (e.g. Dawson, 1964) which assumes that the velocity varies according to $\frac{\ell V}{a}$, where ℓ is the distance of the point of observation from the focal point and is constant, a is the distance of the plasma front from the focal point and increases with time, and V is the velocity of the plasma front. The observations reported in paper I show that V is constant with time, and therefore $\frac{\ell V}{a}$ decreases with time. A possible mechanism for the continued acceleration of the ions is the formation of a sheath - suggested in paper I to explain the fact that the ions do not reach their terminal velocities until some time after the laser pulse is over.

5.3 C V spatial distribution

The spatial distribution of C V in the x, y plane at t = 45 ns is indicated in Fig.5. This result, translated into three dimensions, assuming symmetry about the x axis, indicates that the majority of the C V ions occupy a conical annulus, as shown in Fig.8 at the time t = 45 ns. The form of the annulus in Fig.8 is characteristic of the

plasma at all times though the dimensions vary, e.g. at later times the cone is larger and has moved away from the target surface. It is evident from Fig.3 that the region of C VI emission is within C V and this has been illustrated in Fig.8, and also that the regions of C IV - I come in sequence beyond C V.

It is known that in a laser produced plasma the more highly stripped ions are the first to appear (e.g. Schwob et al. 1970) and have the highest velocities (e.g. Langer et al. 1966) and this has been related to the fact that the greater part of the laser energy is absorbed at the leading edge of the plasma. The present results (Figs.3 and 8) extend this idea by showing that the regions which receive progressively smaller energy, both along and at right angles to the target normal are regions of progressively lower ion stage. It is interesting to note that the dip in C VI on axis (Fig.3) is consistent with this trend since it indicates an increase in electron temperature approaching the x axis.

6. Conclusion

Observations have been made of the intensities of spectral lines to C I to C VI in the spectral range $\lambda\lambda$ 2000 - 6000 Å from a laser produced plasma. Measurements were made both of the variation over space of these intensities (space scans) and of their wavelength profiles modified by the Doppler effect of the ions streaming away from the focal spot (Figs.1, 2 and 3).

The analysis of this data leads to the following picture of the expanding plasma -

(a) each individual species of ion C I - C VI tends to be separated in space;

(b) the region containing the most highly charged ion is at the front of the expanding plasma and is concentrated about the x-axis (an axis which runs from the focal spot normal to the target surface).

(c) lower stages of ionization follow in succession and occupy conical annular regions surrounding the x-axis (CV has been studied in greatest detail - Fig.8).

Measurements of velocity from the Doppler shift in the lines of different ions at different distances from the target normal have led to the plot of velocity versus distance in Fig.4. This shows that the component of the mean streaming velocity at right angles to the target normal increases with distance from the normal. The C V ions have been shown to travel away from the focal spot in approximately straight paths, with velocities along the path in the range $2\text{-}4 \times 10^7$ cm s^{-1} (Fig.6).

Finally velocities have been measured for the ions C IV, V and VI from Doppler shifts in light emitted parallel to the target normal (Fig.7 and Table 2), and are in fair agreement with previous radiation time-of-flight measurements (Boland et al, 1968).

7. Acknowledgements

The assistance given by Mr J. Payne with the operation of the laser is gratefully acknowledged.

REFERENCES

ALLEN, F.J., 1970, J. Appl. Phys., 41, 3048-51.

BASOV, N.G., BOIKO, V.A., DEMENTYEV, V.A., KROKHIN, O.N. and SKLIZHOV, G.V., 1966, Zh. Eksp. Teor. Fiz., 51, 989-1000, [J.E.T.P. 24, 659-66, 1967].

BASOV, N.G., GRIBKOV, V.A., KROKHIN, O.N. and SKLIZKOV, G.V., 1968, Zh. Eksp. Teor. Fiz., 54, 1073-87, [J.E.T.P. 27, 575-82, 1968].

BASOV, N.G., BOIKO, V.A., GRIBKOV, V.A., ZAKHAROV, S.M., KROKHIN, O.N. and SKLIZKOV, G.V., 1969, Ninth International Conference on Phenomena in Ionized Gases, Bucharest, 333; also Akad. Nauk. Doklady, 1248-50, 192, 1970.

BOLAND, B.C., IRONS, F.E. and McWHIRTER, R.W.P., 1968, J. Phys. B: Atom. Molec. Phys., 1, 1180-91.

BYKOVSKII, Yu.A., DOROFEEV, V.I., DYMOVICH, V.I., NIKOLAEV, B.I., RYZHIKH, S.V., and SIL'NOV, S.M., 1968, Zh. Tekh. Fiz., 38, 1194-6. [Sov. Phys.-Tech. Phys. 13, 986-8, 1969].

BYKOVSKII, Yu.A., DEGTYARENKO, N.N., DYMOVICH, V.I., ELESIN, V.F., KOZYREV, Yu.P., NIKOLAEV, B.I., RYZHIKH, S.V. and SIL'NOV, S.M., 1969a, Zh. Tekh. Fiz., 39 1694-6. [Sov. Phys.-Tech. Phys., 14, 1269-71, 1970].

BYKOVSKII, Yu.A., DUBOLADOV, A.G., DEGTYARENKO, N.N., ELESIN, V.F., KOZYREV, Yu.P. and NIKOLAEV, I.N., 1969b, Zh. Eksp. Teor. Fiz., 56, 1819-22. [J.E.T.P., 29, 977-8, 1969]

DAWSON, J.M., 1964, Phys. Fluids, 7, 981-7.

DAWSON, J., KAW, P., and GREEN, B., 1969, Phys. Fluids, 12, 875-82.

DEMTRÖDER, W. and JANTZ, W., 1970, Plasma Phys., 12, 691-703.

DHEZ, P., JAEGLE, P., LEACH, S. and VELGHE, M., 1969, J. Appl. Phys., 40, 2545-8.

ELOY, J.F., 1969, First International Conference on Ion Sources, I.N.S.T.N. Saclay, France, 617-33.

FABRE, E., VASSEUR, P. and BEVERNAGE, G., 1966, Phys. Lett., 20, 381-2.

GREGG, D.W., and THOMAS, S.J., 1966, J. Appl. Phys., 37, 4313-6.

IRONS, F.E., 1971, to be submitted to J. Phys. B.

LANGER, P., TONON, G., FLOUX, F., and DUCANZE, A., 1966, I.E.E.E. J. Quant. Electron. QE-2, 499-507.

OPOWER, H., and BURLEFINGER, E., 1965, Phys. Lett., 16, 37-8

OPOWER, H., and PRESS, W., 1966, Z. Naturf., 21a, 344-50.

OPOWER, H., KAISER, W., PUELL, H., and HEINICKE, W., 1967, Z. Naturf., 22a, 1392-7.

PEACOCK, N.J., and PEASE, R.S., 1969, J. Phys. D: Appl. Phys., 2, 1705-16.

SCHWOB, J.L., BRETON, C., SEKA, W., and MINIER, C., 1970, Plasma Phys. 12, 217-225.

SUCOV, E.W., PACK, J.L., PHELPS, A.V., and ENGLEHART, A.C., 1967, Phys. Fluids, 10, 2035-48.

TONIN, G. and RABEAU, M., 1969, First International Conference on Ion Sources, I.N.S.T.N. Saclay, France, 605-16.

VALERO, F.P.J., GOORVITCH, D., FRAENKEL, B.S., and RAGENT, B., 1969, J. Opt. Soc. Am., 59, 1380-1.

WEICHEL, H. and AVIZONIS, P.V., 1966, App. Phys. Lett., 9, 334-7.

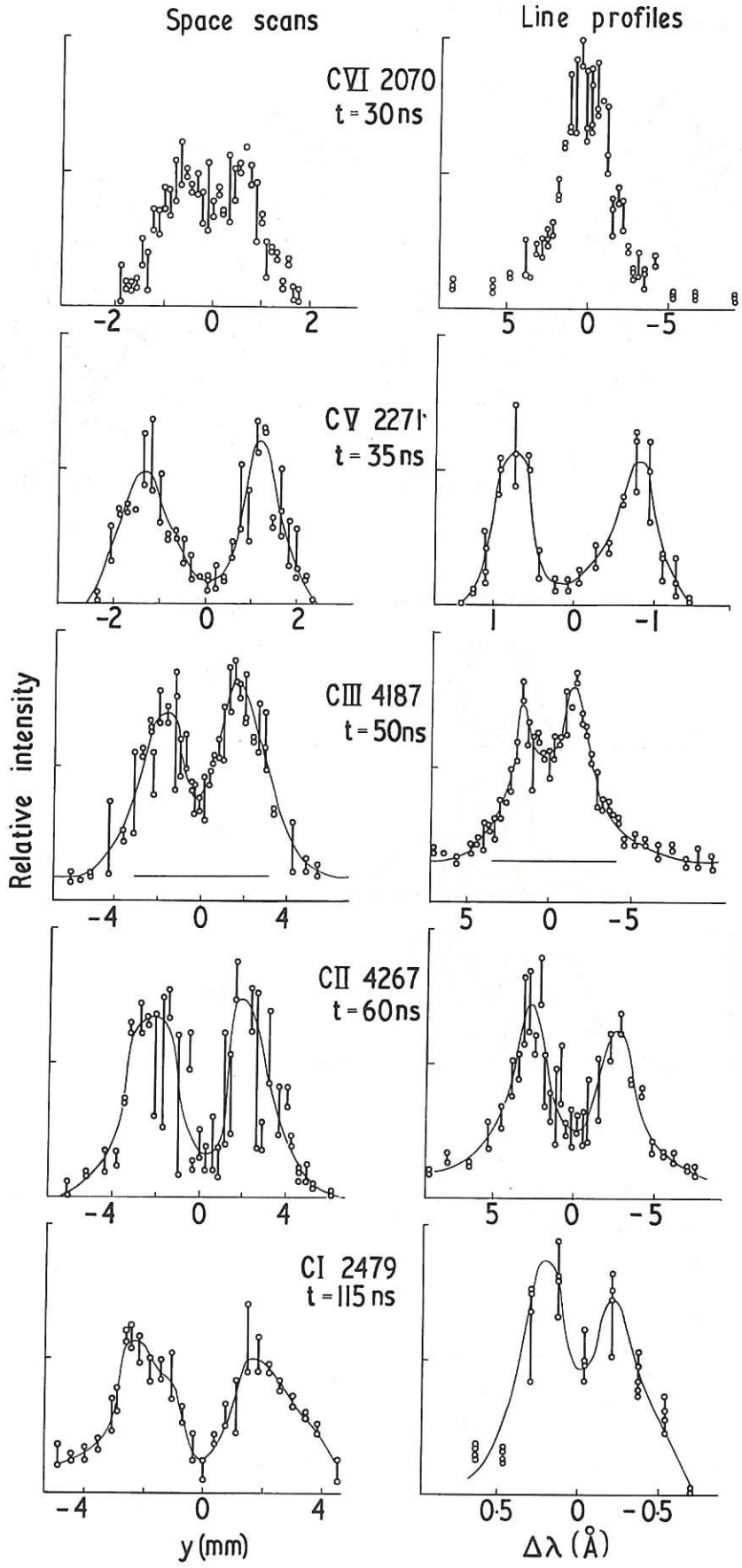

Fig. 1 Examples of space scans and line profiles of C VI, III and II at x = 1.6 mm.

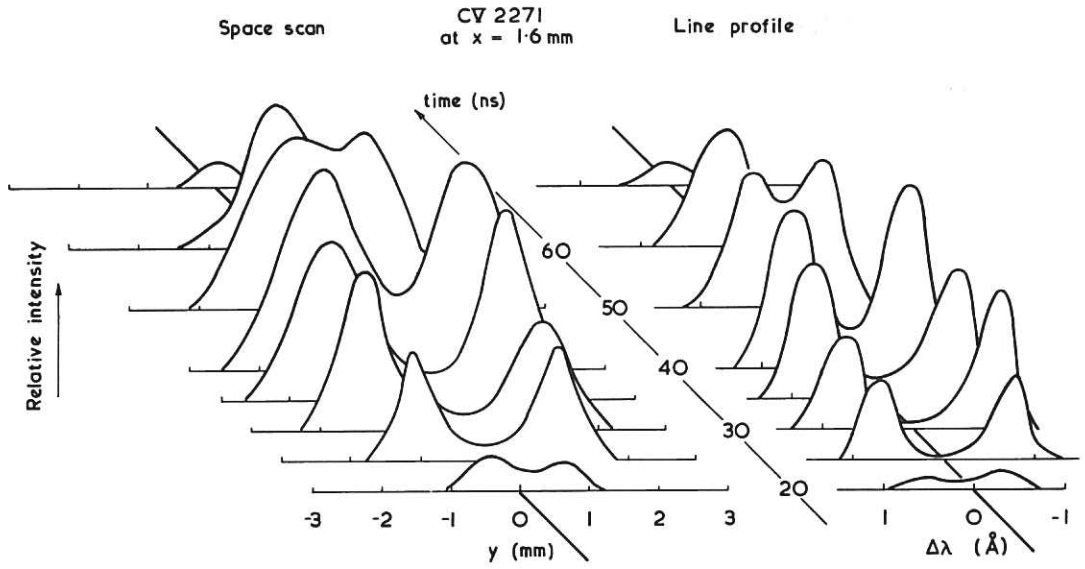

Fig. 2 A time sequence of space scans and line profiles of C V 2271 at x = 1.6 mm

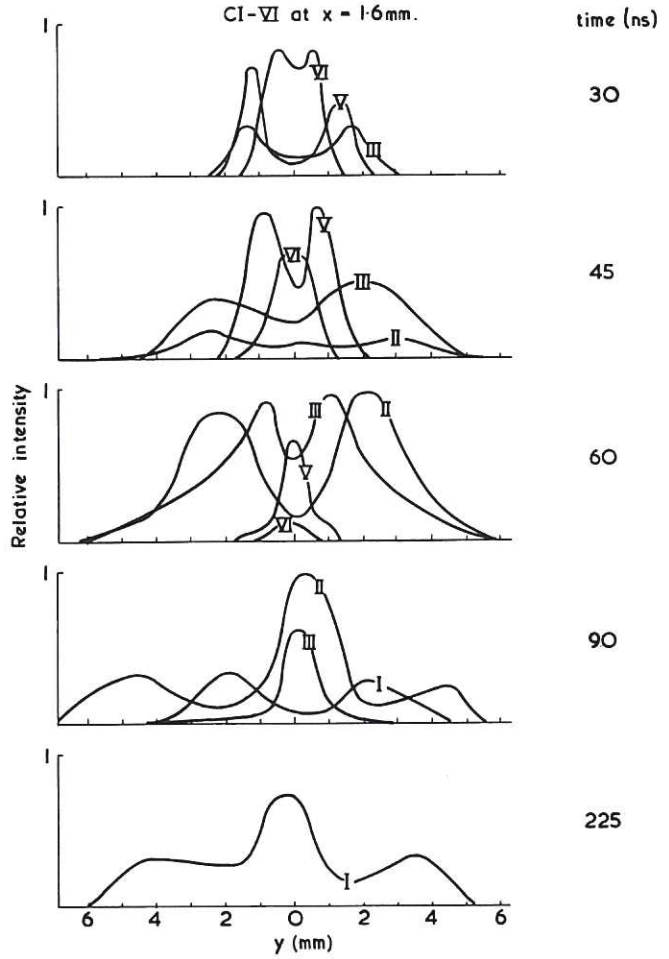

Fig. 3 A time sequence of space scans of C I-VI at x = 1.6 mm

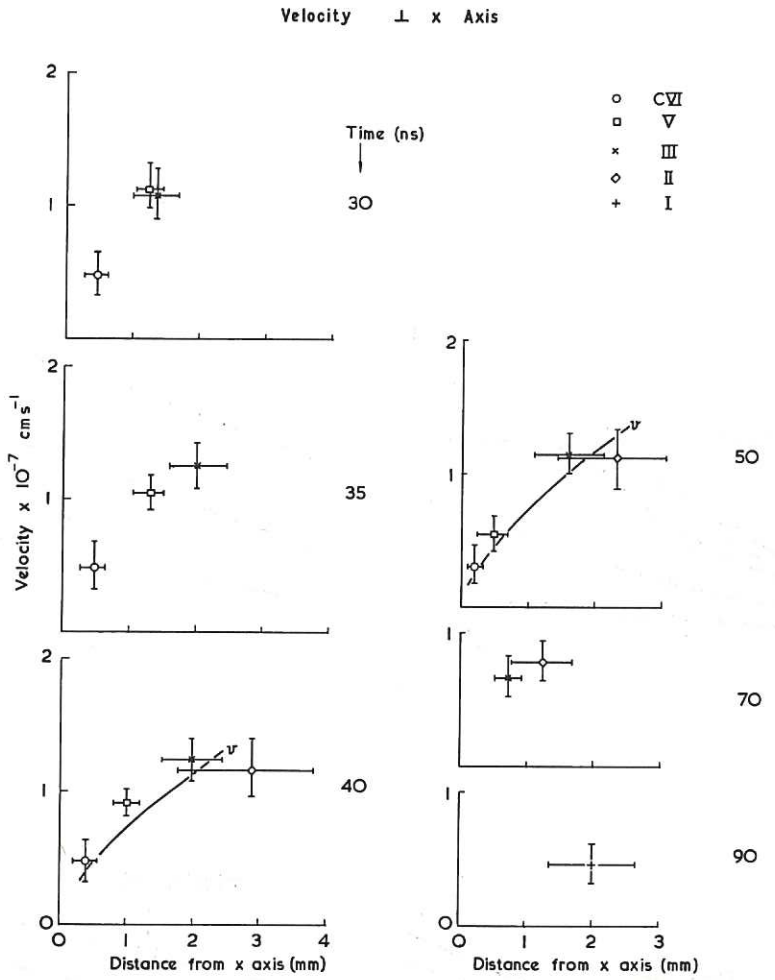

Fig. 4 Graphs showing mean velocity away from the target normal (in the z direction) as a function of distance from the target normal (in the y direction).

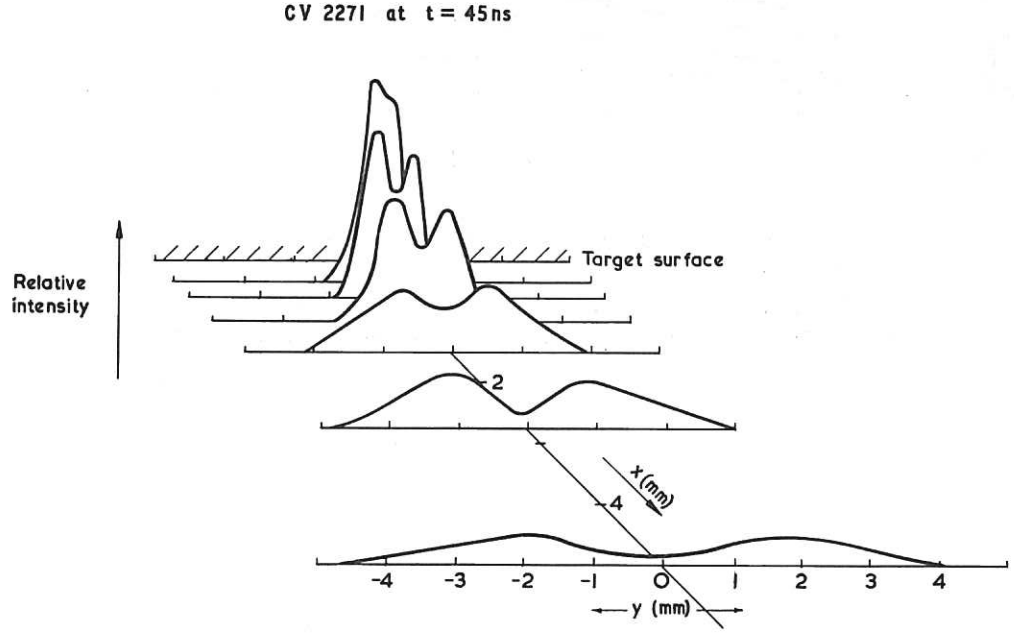

Fig. 5 The distribution of C V 2271 in the x, y plane at t = 45 ns.

CLM-P268

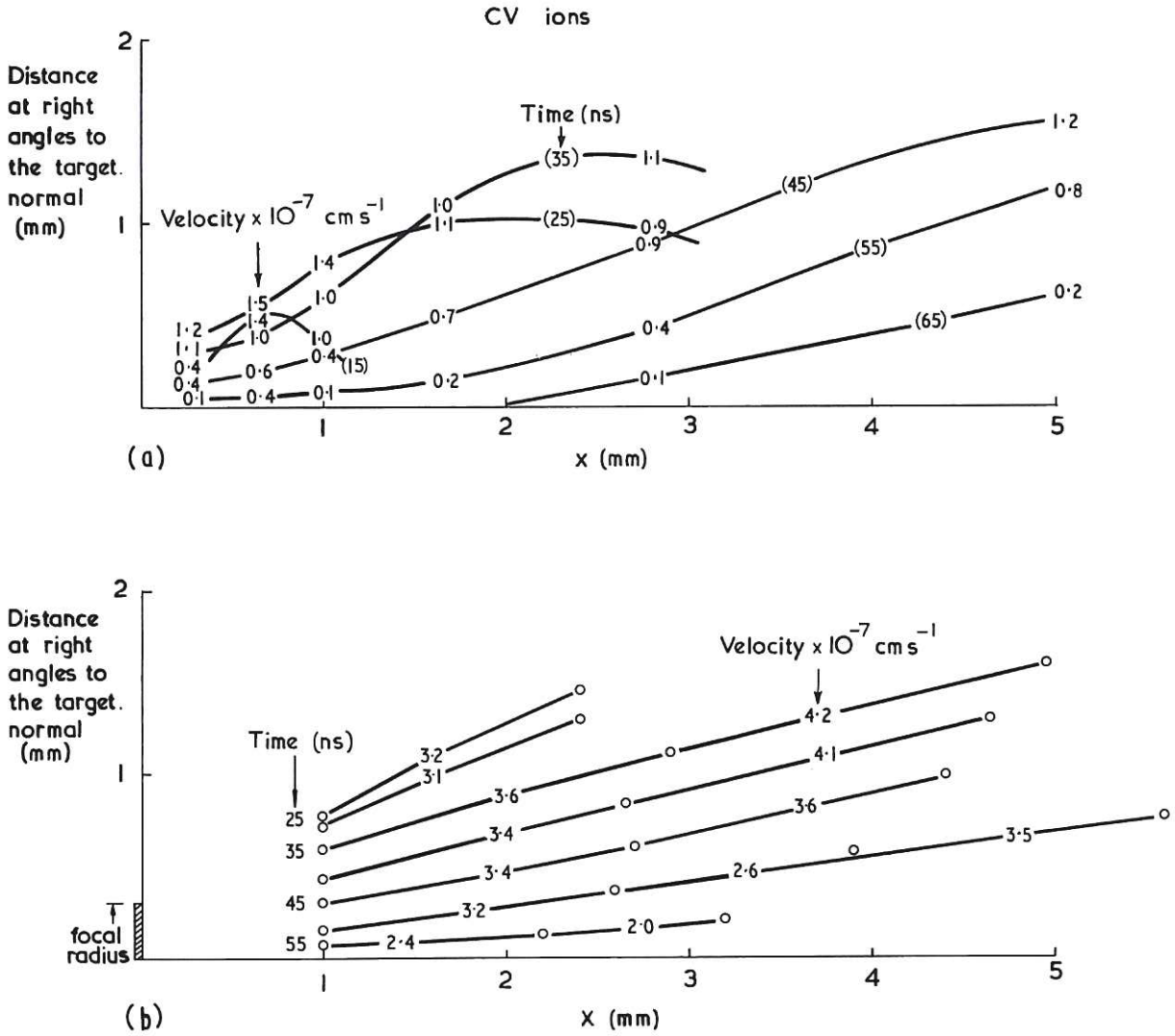

Fig. 6(a) A map showing the distribution of C V 2271 peak intensity in space at a sequence of times (indicated by brackets): included on the curves are velocities away from the x axis;
(b) Ion flight paths, calculated for ions passing the point x = 1.0 mm at the times t = 25(5)55 ns: included on the curves are velocities along the flight paths.

CLM-P268

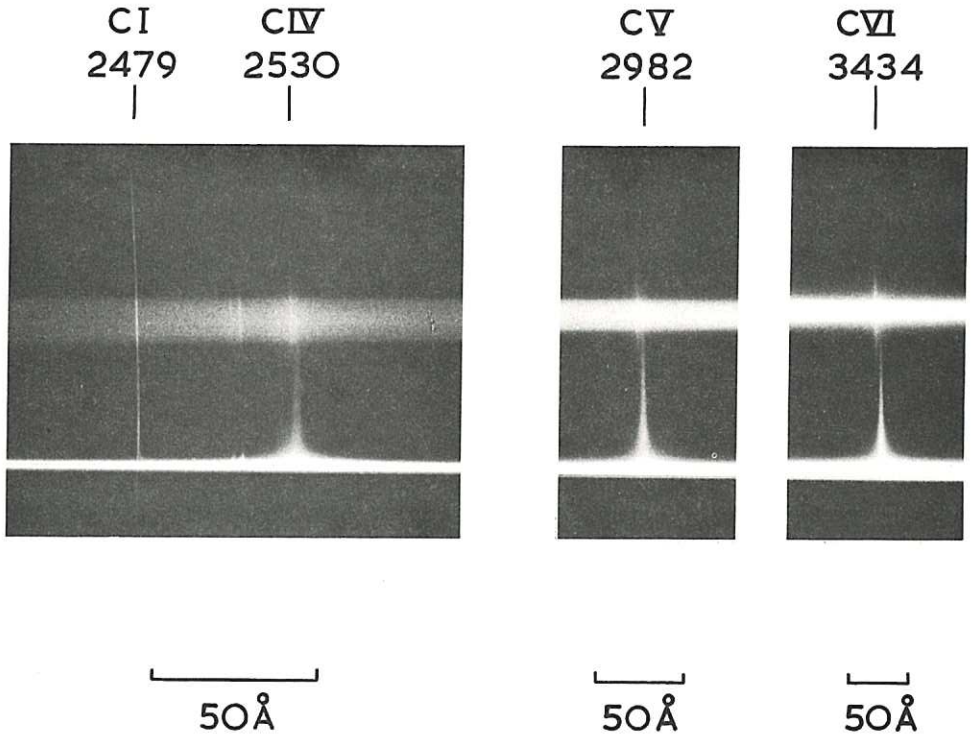

Fig. 7 Spectra showing the Doppler shift in light emitted parallel to the x axis (upper spectrum) compared with the reference spectrum taken at right angles to the x axis (lower spectrum).

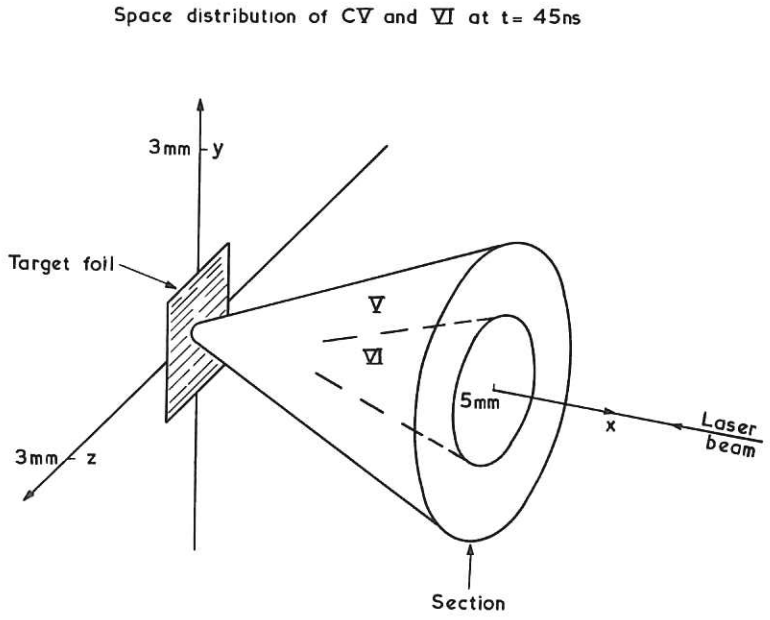

Fig. 8 The spatial distribution of C V and VI from x = 0 - 5 mm at t = 45 ns.